NIH Public Access
Author Manuscript
J Neuropathol Exp Neurol. Author manuscript; available in PMC 2010 February 1.

Published in final edited form as:
J Neuropathol Exp Neurol. 2009 February ; 68(2): 168–178. doi:10.1097/NEN.0b013e3181967df7.

Spinal Cord Injury Reduces the Efficacy of Pseudorabies Virus Labeling of Sympathetic Preganglionic Neurons

Hanad Duale, PhD[1,2,#], **Shaoping Hou, PhD**[1,2,#], **Andrei V. Derbenev, PhD**[2], **Bret N. Smith, PhD**[2], and **Alexander G. Rabchevsky, PhD**[1,2,*]

[1] Spinal Cord and Brain Injury Research Center, University of Kentucky, Lexington, KY 40536-0509

[2] Department of Physiology, University of Kentucky, Lexington, KY 40536-0509

Abstract

The retrograde transynaptic tracer pseudorabies virus (PRV) is used as a marker for synaptic connectivity in the spinal cord. Using PRV we sought to document putative synaptic plasticity below a high thoracic (T) spinal cord transection. This lesion has been linked to the development of a number of debilitating conditions including autonomic dysreflexia. Two weeks after injury, complete T4-transected and/or T4-hemisected and sham rats were injected with PRV-expressing enhanced green fluorescent protein (EGFP) or monomeric red fluorescent protein (mRFP1) into the kidneys. We expected greater PRV labeling after injury due to plasticity of spinal circuitry but 96 hours post-PRV-EGFP inoculation, we found fewer $EGFP^+$ cells in the thoracolumbar gray matter of T4-transected compared to sham rats ($p < 0.01$); Western blot analysis corroborated decreased EGFP protein levels ($p < 0.01$). Moreover, viral glycoproteins that are critical for cell adsorption and entry were also reduced in the thoracolumbar spinal cord of injured versus sham rats ($p < 0.01$). PRV labeling of sympathetic postganglionic neurons in the celiac ganglia innervating the kidneys was also significantly reduced in injured versus sham rats ($p < 0.01$). By contrast, the numbers and distribution of FluoroGold-labeled (intraperitoneal injection) sympathetic preganglionic neurons throughout the sampled regions appeared similar in injured and sham rats. These results question whether spinal cord injury exclusively retards PRV expression and/or transport or whether this injury broadly affects host cell-viral interactions.

Keywords

Intermediolateral column; Neuroplasticity; Pseudorabies virus; Retrograde transsynaptic tracer; Spinal cord injury; Sympathetic nervous system

INTRODUCTION

The central nervous system (CNS) is composed of complex networks of synaptically linked neurons. The development and use of neurotropic viruses as an alternative to traditional tract tracing tools have greatly enhanced our understanding of complex neuronal circuitry, particularly the innervation of thoracic and abdominal viscera (1–7). Despite this progress there is a paucity of knowledge concerning how injury, particularly spinal cord injury (SCI), affects neuronal circuitry. Recent studies in our lab have shown that autonomic dysreflexia, a

*Correspondence and reprint requests to: Alexander G. Rabchevsky, PhD, Associate Professor of Physiology, University of Kentucky, Spinal Cord & Brain Injury Research Center (SCoBIRC), B471, Biomedical & Biological Sciences Research Building, 741 South Limestone Street, Lexington, KY 40536-0509. Telephone: (859) 323-0267; Fax: (859) 257-5737; E-mail: AGRab@uky.edu.
#Both authors contributed equally.

NIH-PA Author Manuscript
NIH-PA Author Manuscript
NIH-PA Author Manuscript

NIH-PA Author Manuscript

NIH-PA Author Manuscript

NIH-PA Author Manuscript

potentially life-threatening hypertensive complication of SCI, correlates with sprouting of both primary afferent and propriospinal fibers at the lumbosacral spinal segment (L6/S1) (8,9). Autonomic dysreflexia is frequently triggered by noxious stimuli below the injury site, particularly by the distension of pelvic viscera (bowel and bladder) (10). This syndrome is characterized by episodic hypertension (sympathetic) and baroreflex-mediated bradycardia (parasympathetic) responses due to initial loss of bulbospinal inhibition of sympathetic output (10,11), which is followed by intraspinal sprouting of nociceptive primary afferent fibers (12). The incidence of dysreflexic hypertension may be the result of altered synaptic inputs to sympathetic preganglionic neurons (SPNs) below the injury site.

To address this hypothesis, we used transynaptic viral tracers (i.e. pseudorabies virus, PRV) that are isogenic with the Bartha strain as markers for synaptic connectivity in central circuits (13). The PRV strain used expresses the reporter gene for enhanced green fluorescent protein (EGFP; PRV-152) or monomeric red fluorescent protein (mRFP; PRV-614) (14–16). The exclusively retrograde transport of PRV Bartha strain occurs in synaptically linked chains of neurons with higher order structures becoming labeled at later time-points (13,17–19). Additionally, viral replication within neuronal cell bodies allows the virus to be a self-amplifying marker; thus second, third and fourth order pre-autonomic neurons that regulate a specific visceral target can be labeled within the spinal cord and higher CNS centers of infected animals.

MATERIALS AND METHODS

Animals and Spinal Surgery

All animal housing conditions, surgical procedures and post-operative care techniques were conducted according to the University of Kentucky Institutional Animal Care and Use Committee and the National Institutes of Health animal care guidelines. Adult female Wistar rats (~200 to 250 g) were anesthetized with a mixture of ketamine (80 mg/kg, i.p.; Fort Dodge Animal Health, Fort Dodge, IA) and xylazine (10 mg/kg, i.p.; Butler, Columbus, OH). The injured groups received either complete T4-transection (n = 26) or a left sided T4-hemisection (n = 12) with a sterile scalpel blade following T3 vertebra laminectomy, in contrast to the sham group (n = 26) which received only T3 laminectomy, as previously described (8,9) (Table 1).

After surgical operations were complete, the erector spinae muscles were sutured with 3-0 Vycril (Ethicon, Sommerfield, NJ), the field was disinfected with povidone-iodine solution (Nova Plus, Irving, TX) and the skin was closed with Michel wound clips (Roboz, Gaithersburg, MD). For post-operative care, animals were given 20 ml lactated Ringer's solution (Baxter Healthcare, Deerfield, IL) and 33 mg/kg cephazolin (Apothecon, Bristol-Myers Squibb, Princeton, NJ) subcutaneously immediately after surgery, and for injured rats twice daily for up to 10 days to maintain hydration and control bladder infection. Buprenorphine (0.035 mg/kg; Reckitt Benckiser, UK) was also administered subcutaneously once after recovery from anesthesia and twice daily for the next 3 days to control post-operative pain. Bladders of injured rats were manually expressed twice daily until automatic bladder-emptying reflex developed at about 10 days post-injury.

PRV Injections

Two weeks after T4-transection, T4-hemisection and sham laminectomy, animals were re-anesthetized with a mixture of ketamine (80 mg/kg, i.p.) and xylazine (10 mg/kg, i.p.) and a laparotomy was performed to expose the abdominal and pelvic contents. With the aid of a dissecting stereomicroscope, 3 μl of PRV-152 (green, 10^8 pfu/ml) were injected into the left kidney of sham (n = 18) and T4-transected (n = 18) rats at 3 sites (1 μl/site) using a 30 gauge Hamilton syringe (Hamilton, Reno, NV) (Table 1). Injections were uniformly placed at sites

NIH-PA Author Manuscript

NIH-PA Author Manuscript

NIH-PA Author Manuscript

on the longitudinal midline of the convex surface of the kidney (5). Injection sites were located by dividing this midline in thirds and injecting at the rostral and caudal end of the middle third. Alternatively, 3 μl of PRV-614 (red, 10^8 pfu/ml) were injected similarly into the left kidney of sham (n = 3) and T4-transected (n = 3) rats at three sites as a control for reporter gene expression (Table 1). For the T4-hemisected rats, 3 μl of PRV-152 (n = 3) and 3 μl of PRV-614 (n = 3) were injected into both the left and right kidneys, respectively (Table 1). To control for potential injury-mediated reporter gene expression, the T4-hemisection paradigm was reversed (e.g. 3μl of PRV-152 (n = 3) and 3 μl of PRV-614 (n = 3) into both the right and left kidneys, respectively) (Table 1). For distal colon injections, the rostral section of the exposed distal colon was elevated and packed off with gauze. A total of 12 μl PRV-152 was injected at 6 sites (2 μl/site) in sham (n = 3) and T4-transected rats (n = 3) using a 30-gauge Hamilton syringe with a sharp beveled tip into the ventral and lateral surfaces of the distal colon 25–40 mm from the anus (20). The needle was run into the viscus wall tangentially to the surface beneath the serosa and either over or into the muscle layer, taking care not to penetrate into the lumen. The needle was inserted 4 to 10 mm and withdrawn 1–2 mm before the virus solution was slowly injected (20). The needle was held in place for 5 minutes and slowly withdrawn under a dry cotton-tipped stick to absorb reflux; this was followed by lavage of the peritoneal space with sterile saline. Injection sites were sealed with a drop of tissue adhesive (3M Vetbond™, St. Paul, MN). To control for PRV specificity, naive rats (control; n = 2) received an intraperitoneal injection of 3 μl of PRV-152 (Table 1). Materials that came into contact with PRV during surgery were cleaned with Clorox bleach (0.05%) solution and properly discarded as biohazard materials. Animals were maintained in a biosafety level 2 facility (72 hours, 84 hours, or 96 hours) until euthanasia prior to perfusions fixation for histology or rapid isolation of fresh spinal tissues for molecular biology. One week prior to perfusion, selected sham (n = 2) and injured (n = 2) rats were given an intraperitoneal injection of Fluoro-Gold (0.2 ml of 1.5% in saline; Biotium, Hayward, CA) to label all sympathetic preganglionic neurons in the intermediolateral cell column (21).

Perfusion and Tissue Processing

Animals designated for histology (n = 58; Table 2) were overdosed with sodium pentobarbital (150 mg/kg; Abbott, Chicago, IL) and perfused transcardially with 0.1 M phosphate buffered saline (PBS), pH 7.4, followed by 4% paraformaldehyde in PBS. The spinal cord from the conus medullaris to the transection site was removed, post-fixed for 4 hours, rinsed in 0.2 M phosphate buffer (PB) overnight, and cryoprotected for at least 48 hours in 20% sucrose in 0.1 M PBS. The caudal and rostral limits of the dissected spinal cords sampled were between 0.5 mm rostral of the conus medullaris (~S4) to 6 cm rostral at the T5 segment. The cords were then divided into two 3 cm portions of caudal (S4-T13; lumbosacral) and rostral segments (T12-T5; thoracic) and embedded in gum tragacanth (Sigma-Aldrich, St. Louis, MO) in 20% sucrose/PBS for cryosectioning, as previously detailed (9). Both thoracic and lumbosacral segments of cord were serially cryosectioned in the longitudinal, horizontal plane at 50 μm and consecutively mounted onto glass slides (Superfrost plus, Fisher Scientific, Pittsburgh, PA) in 5 series of 5 slides. This rendered 250 μm separations between adjacent serial sections within a series on each slide (9).

Immunohistochemistry

For anti-PRV double immunostaining with PRV-614, slides with mounted longitudinal sections were thawed and pre-incubated in 0.1 M PBS containing 0.5% Triton-X and 5% normal donkey serum (Vector Laboratories, Burlingame, CA) for 1 hour, followed by incubation with rabbit anti-PRV 132 (1:1000; Courtesy of Dr. Patrick Card) in same buffer overnight at 4°C. The slides were then rinsed before applying goat anti-rabbit conjugated to AMCA (Jackson ImmunoResearch Laboratories, West Grove, PA; 1:200) for 3 hours at room

NIH-PA Author Manuscript

NIH-PA Author Manuscript

NIH-PA Author Manuscript

temperature. After final rinses, slides were coverslipped using Vectashield mounting medium (Vector) and sealed with Cutex nail hardener (Jackson, WY).

Quantification of PRV-152+ Cells in the Spinal Cord

For PRV-152$^+$ cell quantification after 96 hours post-inoculation, our region of interest was the caudal 2 cm of the thoracic spinal segments, corresponding to T8-T13 of sham (n = 4) versus T4-transected rats (n = 4) (Table 2). Previous studies had shown that EGFP labeledcells following PRV-152 inoculation into the kidneys were mainly distributed from T6-T13, with the highest cellular distribution restricted to T8-T13 (22–24). Serial longitudinal, horizontal sections containing the dorso-ventral extent of the intermediolateral column, which incorporates the majority of SPNs, were selected. To avoid counting the same cell twice, every other collected serial section was used; thus the sections were separated by 100 μm. This corresponded to quantifying 3 alternating serial sections within the intermediolateral column. All quantifications were conducted in a blinded fashion using the Bioquant® image analysis program (Nova Prime, V6.70.10; Bioquant Image Analysis Corp., Nashville, TN) using established methods (9). In brief, under an Olympus BX51 fluorescence microscope (Olympus Corp. Melville, NY), live images corresponding to bilateral gray matter regions in our area of interest (T8-T13) were circumscribed at 4x magnification (10x eye piece) and images captured using an Optronics digital video camera (Optronics Corp., Goleta, CA). This corresponded to approximately 5.8 mm^2 for shams and 6 mm^2 for injured cords, depending upon dorso-ventral plane. In conjunction with Microcode II stage encoders (Boeckler Instruments, Tucson, AZ) and using a 60x oil immersed objective (10x eye piece), all EGFP$^+$ cells within the circumscribed area through the section plane were counted. Although counting all objects within a circumscribed area is a valid and efficient method, it is however prone to over-counting (25). To minimize over-counting we used the correction factor first computed by Abercrombie (1946); T/T + h, where T = section thickness and h = mean diameter of the objects along the z- axis (25,26). Photomicrographs in all figures were optimized for final production by adjusting only the brightness and contrast using Adobe Photoshop 7.0 (Adobe Systems Inc., San Jose, CA). All graphs were created with DeltaGraph 5.4 (Red Rock Software, Inc., Salt Lake City, UT).

Spinal Cord Tissue Extraction and Protein Assay

Injured and sham animals designated for Western blot analysis (n = 8, Table 2) were euthanized with CO_2 and decapitated at 96 hours following PRV-152 inoculation into the left kidney. The spinal cords (T5-conus medullaris) were rapidly removed (27) and placed on an ice-cold dissecting plate containing pre-cooled Triton lysis buffer pH 7.4 (1% triton, 20 mM Tris HCl, 150 mM NaCl, 5 mM EGTA, 10 mM EDTA, 10% glycerol) with protease inhibitors (Complete Mini™ Protease Inhibitor Cocktail tablet). The spinal cords were dissected into 2-cm segments, centered between the T8-T13 spinal rootlets, and homogenized in 1 ml of Triton lysis buffer with protease inhibitors. Samples were then briefly sonicated and vortexed at 14,000 rpm for 30 minutes at 4°C, and the supernatants were collected for protein assay. Protein concentration was determined by Bio-Rad DC Protein Assay (Bio-Rad, Hercules, CA), with sample solutions diluted to contain 1 mg/ml of protein for immunoblotting.

Celiac Ganglia Tissue Extraction and PRV+ Neuronal Quantification

The celiac plexus is situated around and between the celiac artery and the superior mesenteric artery and extends dorsally between the adrenal glands and the cranial half of the kidneys (28). The left celiac ganglion is crescent shaped and lies on the lateral side of the celiac and superior mesenteric artery; the right celiac ganglion is triangular, smaller than the left one, and lies dorsal to the inferior vena cava (28). To facilitate visualization and isolation of the PRV infected ganglia, injured, and sham animals were euthanized with CO_2 and immediately

NIH-PA Author Manuscript

NIH-PA Author Manuscript

NIH-PA Author Manuscript

decapitated. Both the left (PRV $^{+}$) and right (PRV^{-}) celiac ganglion were isolated and submerged in ice-cold 4% paraformaldehyde in 0.1M PBS for 48 hours. Post-fixed ganglia were rinsed in 0.2 M PB overnight and cryoprotected for at least 48 hours in 20% sucrose in 0.1 M PBS. In addition the spinal cords were also extracted, post-fixed and processed as described to verify CNS labeling. As described above, the ganglia were embedded in gum tragacanth and serially cryosectioned in the longitudinal, horizontal plane at 20 μm and consecutively mounted onto glass slides in 5 series of 5 adjacent slides. This rendered 100 μm separations between serial sections within a series on each slide (9). To verify putative ganglionic neurons, selected serial sections were stained with cresyl violet. In brief, chosen slide series were subjected to sequential rehydration followed by cresyl violet stain (Cresyl Violet acetate, Sigma) for 5 minutes, followed by a sequential dehydration phase. Stained sections were maintained in Citrisolv (Fisher Scientific) to clear excess cresyl violet and subsequently coverslipped with Permount (Fisher Scientific) mounting medium.

For quantification of PRV-152^{+} sympathetic postganglionic neurons in the left celiac ganglion, a total of 12 rats (Table 2) were used and divided into injured (n = 6) and sham (n = 6) groups. These groups were further subdivided by inoculation time (48 hours, n = 6 (including injured and sham); 72 hours, n = 6). Preliminary data revealed that PRV labeling of the left celiac ganglion (right celiac ganglion acted as a negative control) was optimal at 72 hours versus 48 hours post-viral inoculation into the left kidney. Consequently, the total number of PRV-152^{+} cells in the left celiac ganglion at 72 hours post-left kidney inoculation was quantified using the Bioquant® image analysis program, similar to quantification in the thoracic cord. Notably, however, due to the small size of the ganglia we quantified each sequential section throughout adjacent serial slides. For each section, the cross-sectional area of the entire left ganglion was circumscribed at 4x magnification (10x eye piece) and images captured using an Optronics digital video camera. Only a subpopulation of celiac sympathetic postganglionic neurons innervate the kidneys, so all EGFP^{+} cells within the circumscribed area of every section was counted using a 60x oil immersed objective (10x eye piece). To correct for possible over-counting, we employed the Abercrombie factor as described above.

Western Blot Analysis of PRV-152 and PRV-Associated Proteins VP-5 and gB-C

To measure the relative expression levels of EGFP (there is no commercially available antibody against m RFP1), PRV-associated major capsid coat protein (VP-5), and glycoproteins B-C (gB-C), spinal cord samples (50 μg, 40 μg and 40 μg, respectively) corresponding to both injured (n = 4) and shams (n = 4) were run on an SDS/PAGE Precast gel (EGFP: 12% Bis-Tris Criterion™ XT Precast gel, Bio-Rad; gB-C and VP-5: 4–12% Bis-Tris Criterion™ XT, Bio-Rad), using established methodologies (29). Afterwards, the proteins were transferred onto a PVDF membrane (Immuno-blot PVDF membrane-0.2 μm, Bio-Rad) using a semi-dry electro-transferring unit set at 15 V for 15 minutes. Preliminary experiments established protein concentration curves in order to ensure that quantified bands were in the linear range as measured with the Li-Cor Odyssey Infrared Imaging System (Li-Cor Biotechnology, Lincoln, NE). The membranes were incubated in Tris-buffered saline (TBS, pH 7.4) blocking solution with 5% milk (Great Value™ instant non-fat dry milk, Wal-Mart) for 1 hour at room temperature. For the detection of EGFP, a rabbit polyclonal anti-GFP antibody (-ab290, Abcam, Cambridge, MA) was used at a dilution of 1:1000 in TBS-Triton (TBST) blocking solution with 5% milk for overnight at 4°C. A goat anti-rabbit secondary conjugated to an infrared dye (1:5000, IRDye800CW, Rockland Immunochemicals, Gilbertsville, PA) was then applied for 1 hour at room temperature. After drying, the membranes were then imaged and quantified using the Li-Cor Odyssey Infrared Imaging System. To detect PRV associated VP-5 (154 KDa) and gB-C proteins (NB: the glycoproteins B and C have similar size band ~70 KDa), a rabbit polyclonal anti-PRV (RB132, kindly donated by Dr. Patrick Card, University of Pittsburgh) was used at a dilution of 1:1000 in TBST blocking solution with 5% milk overnight

NIH-PA Author Manuscript

NIH-PA Author Manuscript

NIH-PA Author Manuscript

at 4°C. A goat anti-rabbit secondary conjugated to an infrared dye (1:5000, IRDye800CW, Rockland Immunochemicals) was then applied for 1 hour at room temperature. To standardize protein loading, EGFP, VP-5 and/or gB-C immunoreactive PVDF membranes were subsequently stripped (i.e. remove primary and secondary antibodies from the membrane) and re-probed with mouse monoclonal anti β-actin (1:500, Sigma). In brief, the PVDF membrane was bathed in a stripping buffer containing 25 mM glycine-HCl, pH 2, and 1% SDS for 1 hour and replaced with fresh buffer every 15 minutes. After stripping, the PVDF membrane was washed extensively in PBS + 0.1% Tween-20 (3 × 5 minutes) and subsequently incubated for 1 hour in TBS blocking solution with 5% milk at room temperature. For the detection of β-actin, mouse monoclonal anti-β-actin was used at a dilution of 1:500 in TBST with 5% milk for overnight incubation at 4°C. A goat anti-mouse secondary conjugated to an infrared dye (1:5000, IRDye800CW, Rockland Immunochemicals) was then applied for 1h at room temperature and the β-actin$^+$ PVDF membrane visualized with Li-Cor Odyssey Infrared Imaging System.

Statistical Analysis

Statistical analyses between spinal-transected and non-transected rats were performed using Stat-View (SAS Institute, Cary, NC). Unpaired Student t-test was used between non-transected and injured groups. Significance throughout all experiments was set at $p < 0.05$. Data are represented as mean ± SD.

RESULTS

Effects of T4-Spinal Transection on EGFP/RFP Expression Patterns of Neurons in the Thoracolumbar Spinal Cord

The PRV cellular labeling pattern observed in the thoracolumbar spinal cord following PRV-152 injection into the left kidney includes the labeling of ipsilateral SPNs and interneurons at 72 hours post-inoculation (Fig. 1A). By 96 hours post-inoculation, there were extensive EGFP$^+$ cells from T6-T13, with the highest numbers concentrated at T8-T13 (Fig. 1B). At 2 weeks following complete T4-transection, however, EGFP$^+$ cells from T8-T13 were markedly reduced compared to sham rats (Fig. 1C, D). Moreover, semiquantitative Western blot analysis of EGFP expression in the thoracolumbar spinal cord showed a significant reduction in injured versus sham rats (F [1,6] = 13.61; $p < 0.01$) (Fig. 2). To rule out the possibility that reduced PRV labeling after injury is limited to specific reporter genes (i.e. EGFP), we injected PRV-RFP into the left kidney of sham versus injured rats and observed a similar outcome as for the PRV-152 paradigm (Fig. 3A, B). Furthermore, anti-PRV immunostaining in the same sections appeared to show fewer labeled neurons in injured versus sham rats at 96 hours post-inoculation (Fig. 3C, D). Conversely, intraperitoneal injection of FluoroGold and subsequent labeling of SPNs throughout the thoracolumbar spinal cord appeared unaltered in sham and injured rats (Fig. 3E, F).

Effects of T4-Spinal Transection on EGFP Expression Patterns of Neurons in the Lumbosacral Spinal Cord

To assess whether SCI differentially affects the sympathetic versus parasympathetic autonomic branches, we injected PRV-152 into the distal colon (T4-transected, n = 3; sham, n = 3), which receives parasympathetic innervation from the sacral parasympathetic preganglionic neurons in the lumbosacral (L6/S1) spinal cord of rats. At 96 hours post-PRV-152 inoculation into the distal colon, there was no qualitative difference in EGFP$^+$ cellular labeling pattern in the L6/S1 spinal cord between sham and injured rats (Fig. 4A, B).

NIH-PA Author Manuscript

NIH-PA Author Manuscript

NIH-PA Author Manuscript

Effects of T4-Hemisection on EGFP/RFP Expression Patterns of Neurons in the Thoracolumbar Spinal Cord

To rule out the possibility of compromised PRV uptake being limited to complete spinal cord transection, left-sided T4-hemisected rats were injected with PRV-152 (green; injured side) and PRV-614 (red; intact side) into the left and right kidneys, respectively (Table 2). At 72 hours (n = 2) and 84 hours (n = 2) post-inoculation, spinal cord tissue ipsilateral to the injury (left side) appeared to show fewer PRV-152$^+$ cells compared to the PRV-614$^+$ cells in the contralateral uninjured spinal cord (Fig. 4C, D). Similarly, when the injection paradigm was reversed (i.e. PRV-614 [injured side] into the left kidney and PRV-152 [intact side] into right kidney) we observed the same phenomena as described above at 72 hours (n = 2) and 84 hours (n = 2) post-inoculation (data not shown). Notably, in both injection paradigms at 96 hours post-inoculation (total; n = 4), we observed considerable intermingling of PRV-152$^+$ and PRV-614$^+$ cells in the ipsilateral and contralateral thoracolumbar spinal cord (data not shown).

Expression Levels of EGFP and PRV-Associated Proteins in the Thoracolumbar Spinal Cord

The significant reduction in EGFP$^+$ cells in the thoracolumbar spinal cord of injured rats after left kidney PRV injection (Fig. 2) was corroborated by Western blot analysis that showed significant decrease in EGFP protein levels ($p < 0.01$) (Fig. 5A, B). This reduced EGFP expression could be the result of either injury-induced disruption in transcription and translational mechanisms or reduced viral uptake at the synapses. Since immunostaining for PRV appeared reduced (Fig. 3C, D), the most likely explanation is reduced viral uptake, Uptake of PRV initially depend upon the adsorption of virions to a heparin sulfate proteoglycan moiety on the host cell surface, which is mediated by glycoprotein C (gC) (30), while glycoprotein B and D (gB and gD) are involved in cell surface penetration (31). Analysis of viral gB-C protein levels at 96 hours post-inoculation showed a significant reduction ($p < 0.01$) in injured compared to sham rats (Fig. 5C, D). Importantly, VP-5, a critical protein that is involved in viral capsid formation (and thus viral assembly), was also significantly reduced ($p < 0.01$) in injured versus sham rats (Fig. 5E, F).

Effects of T4-Spinal Transection on EGFP Expression Patterns of Neurons in the Celiac Ganglia

Because PRV labeling of postganglionic neurons in the spinal cord was retarded by SCI, we sought to determine whether PRV transport in the sympathetic postganglionic neurons that innervate the kidneys was also affected by SCI. Therefore, PRV-152 was injected into the left kidney to label sympathetic postganglionic neurons in the left celiac ganglion. PRV-152 expression patterns in the left celiac ganglion indicated that a subpopulation of celiac neurons was labeled in both injured and sham tissue samples (Fig. 6A, B). This was expected since the ganglia also innervate other organs. Notably, we did not observe any PRV labeling in the right celiac ganglion (i.e. the negative control). Quantitative analysis revealed significantly less PRV labeling in the left celiac ganglion of injured versus sham rats at 72 hours post-viral inoculation ($p < 0.01$) (Fig. 6C).

DISCUSSION

Numerous studies have demonstrated the utility of PRV as a transsynaptic tracer in the rats CNS (5,14,16,32) but SCI–induced plasticity of kidney-related sympathetic and colon-related parasympathetic, neural pathways has not been studied previously using PRV. The present study used transsynaptic labeling with PRV to investigate putative axon remodeling after SCI, a crucial component in the development of autonomic dysreflexia (8,9).

NIH-PA Author Manuscript

NIH-PA Author Manuscript

NIH-PA Author Manuscript

PRV Labeling in the Thoracolumbar Spinal Cord

The patterns of labeling in the thoracolumbar (T6-L1) spinal cord of sham rats following PRV inoculation into the left kidney at 72, 84 and 96 hours post-injection were comparable to those in previous studies (22,24). At 72 hours post-inoculation, PRV labeling was restricted predominately to second order sympathetic preganglionic neurons; by 84 hours, third order interneurons were labeled; and by 96 hours the entire thoracolumbar cord appeared labeled (Fig. 1A, B); discrete regions of the lumbosacral cord were also labeled (unpublished observation). By contrast, the pattern of PRV labeling in these regions following chronic SCI was dramatically altered. We analyzed spinal tissues infected after 96 hours rather than 84 hours or 72 hours because the Western blot signals from the earlier time points were insufficient for quantification. Counting of PRV^+ cells in fixed spinal tissues was also conducted in tissue following 96 hours post-PRV inoculation to maintain consistency. The marked reduction in PRV labeling corresponded with decreased expression of viral glycoproteins (gB-C) that facilitate viral adsorption and entry into the cell in sham versus injured rats. In contrast, intraperitoneal injection of FluoroGold and subsequent labeling pattern of SPNs throughout the thoracolumbar spinal cord appeared unchanged in sham versus injured rats (Fig. 3E, F), indicating that the reduced PRV was not due to loss of autonomic motor neurons in injured spinal cords. The differences observed between FluoroGold and PRV labeling in the thoracolumbar spinal cord may be due to differential uptake mechanisms, that is, FluoroGold is taken up via pinocytosis whereas PRV uptake is receptor-mediated. We cannot rule out the possibility, however, that altered intracellular transport and/or transcription/translation of viral protein products also contributed to the attenuation of PRV labeling following injury. Accordingly, in the left-sided T4-hemisection paradigm we observed at 72 hours and 84 hours but not at 96 hours post-PRV inoculation, a marked reduction in PRV-152 labeling in the ipsilateral spinal cord compared to the contralateral uninjured side labeled with PRV-RFP (Fig. 4C, D). Moreover, this observation was independent of the PRV reporter gene expressed (i.e. PRV-RFP or PRV-152) (Figs. 1C, D, 3A, B).

PRV Labeling in the Celiac Ganglia

SCI leads to disruption of the descending spinal cardiovascular pathways resulting in sympathetic hypoactivity and unopposed prevalence of the intact vagal parasympathetic control (33). Sympathetic hypoactivity results in low resting blood pressure, loss of regular adaptability of blood pressure, and disturbed reflex control (34). The loss of descending supraspinal sympathetic excitatory and inhibitory control (35), in addition to morphologic alterations of the sympathetic preganglionic neurons, could account for reduced uptake of PRV from the peripheral nervous system (36). Anecdotal evidence suggests that postganglionic neurons are altered by SCI, since reduced sympathetic activity is associated with low plasma adrenaline and noradrenaline levels (37,38). The celiac ganglia provide the principle autonomic (i.e. sympathetic) innervation of the kidneys (39) and quantitative analysis of left celiac ganglion following viral inoculation into the left kidney revealed significantly less PRV labeling of sympathetic postganglionic neurons in injured compared to sham rats. These data imply that sympathetic postganglionic neurons are also susceptible to the effects of centrally mediated injury. A plausible explanation for the perturbation of PRV uptake at the postganglionic synapse is reduced neuronal activity due to diminished afferent input from denervated preganglionic neurons, which may adversely influence the expression profile of PRV-specific cell receptors.

PRV labeling in the Lumbosacral Spinal Cord

Since painful bowel distention is one of the main triggers of autonomic dysreflexia (10,11), we sought to identify whether the parasympathetic innervation of the distal colon is similarly altered by SCI as sympathetic innervation of the kidneys. Notably, in 1989 de Groat et al had

NIH-PA Author Manuscript

NIH-PA Author Manuscript

NIH-PA Author Manuscript

demonstrated that unilateral parasympathetic denervation of the cat bladder caused significant reorganization, (i.e. hyperactivity), of the sympathetic efferent output to the pelvic ganglion, leading to the conversion of sympathetic inhibitory to excitatory input to the denervated bladder (40). Following PRV-152 inoculation into the distal colon, we observed no qualitative difference in the PRV labeling pattern of colon-related (i.e. sacral parasympathetic preganglionic) neurons in sham versus injured rats. This lack of difference may indicate the differential affect of SCI on the sympathetic versus parasympathetic branches of the autonomic nervous system. Alternatively, our findings following PRV injection into the distal colon might be explained by the distance from the injury. Krassioukov and Weaver showed that following complete mid-thoracic transection, injury-mediated morphological changes in the SPN continued as far as 6 spinal segments caudal from the injury site (36), whereas in our paradigm approximately 15 spinal segments separated the T4-transection site and the lumbosacral spinal cord. Importantly, Vizzard *et al* assessed the relative contribution of both the spinal (i.e. sympathetic) and vagal (i.e. parasympathetic) pathways in PRV transport to the brain following mid-thoracic (T8) transection (41). Following PRV inoculation into the distal colon, PRV-infected cells were detected in the caudal medullary regions (vagal pathway) in both sham and injured rats; however, labeling in the Barrington's nucleus (spinal pathway) (42) was eliminated or significantly reduced. Regrettably, the study by Vizzard et al did not assess PRV labeling patterns in the lumbosacral spinal cord following SCI. Nevertheless, in agreement with the current study, this infers differential influences of SCI on the distinct autonomic pathways that regulate pelvic visceral function.

Methodological Considerations

Modern anatomical studies of neuronal interactions and fiber pathways in the CNS rely on the use of transneuronal tracers that transport through live axons in the anterograde or retrograde direction. Conventional neuronal tracers such wheat germ agglutinin conjugated to horseradish peroxidase (43) and fast blue (44) are popular because they offer several technical advantages including, high sensitivity and relatively simple methodology but these methods have limitations, including weak labeling, color fading, and non-specific spread to adjacent cells (45,46). A major advantage of using recombinant viruses as tracers is their ability to migrate transsynaptically in the retrograde direction and replicate within the neuron. Thus, they function as self-amplifying cell markers, ensuring a high signal to noise ratio using fluorescent transgene expression or standard immunohistochemistry procedures, allowing dual immunolabeling of virus and neuronal phenotype in the same reaction. Nevertheless, recombinant viruses as tract tracers have limitations. For example, the appropriate receptor/ligand for viral adsorption and entry into the cell needs to be present in for effective labeling. As demonstrated in the current study, the receptor/ligand density and binding kinetics might be changed in CNS injury. Indeed, with the advent of viral-mediated gene therapy, numerous studies have touted its potential therapeutic value in various pathological conditions (47–49). In view of the present study, care should be taken when assessing results using such an approach in spinal injury models, not only in terms of gene expression but also viral uptake. The broader implication is that gene therapy strategies for treating the injured spinal cord must take into consideration that reduced expression levels of cell receptors required for viral adsorption and entry may limit the efficacy of transgene expression, and hence mitigate potential neuroanatomic and/or behavioral outcome measures.

Collectively, our results demonstrate that, after chronic SCI, kidney-related sympathetic preganglionic and postganglionic neurons undergo physiological changes that significantly retard PRV but not FluoroGold uptake. In contrast, the uptake of PRV by colon-related parasympathetic neurons in the lumbosacral spinal cord appeared unaffected by SCI. An important consideration is whether SCI exclusively retards PRV expression or other host cell-

NIH-PA Author Manuscript

NIH-PA Author Manuscript

NIH-PA Author Manuscript

viral interactions and/or whether axonal transport in sympathetic circuits only is altered after SCI.

Acknowledgments

We thank Drs. Lynn Enquist (Princeton University), Peter Strick, and Patrick Card at the Center for Neuroanatomy with Neurotropic Viruses (CNNV; University of Pittsburgh) for providing reagents and technical expertise in the production of the PRV-152. Thanks also to Dr. Roger Tsien (University of California San Diego) for the mRFP1 and Dr. Bruce Banfield (University of Colorado) for the PRV-614. In addition, we are grateful to Drs. James Geddes and George Smith (University of Kentucky) for critical review of the manuscript.

Funded by PVA grant #2561 (H. Duale), NINDS, R01 NS049901 (A.G. Rabchevsky), NIDDK R01 DK056132 (B.N. Smith), and NINDS, P30 NS051220.

References

1. Standish A, Enquist LW, Escardo JA, et al. Central neuronal circuit innervating the rat heart defined by transneuronal transport of pseudorabies virus. J Neurosci 1995;15:1998–2012. [PubMed: 7891147]
2. Jansen AS, Hoffman JL, Loewy AD. CNS sites involved in sympathetic and parasympathetic control of the pancreas: a viral tracing study. Brain Res 1997;766:29–38. [PubMed: 9359584]
3. Hadziefendic S, Haxhiu MA. CNS innervation of vagal preganglionic neurons controlling peripheral airways: a transneuronal labeling study using pseudorabies virus. J Auton Nerv Syst 1999;76:135–45. [PubMed: 10412837]
4. Nadelhaft I, Vera PL, Card JP, et al. Central nervous system neurons labelled following the injection of pseudorabies virus into the rat urinary bladder. Neurosci Lett 1992;143:271–74. [PubMed: 1331903]
5. Tang X, Neckel ND, Schramm LP. Spinal interneurons infected by renal injection of pseudorabies virus in the rat. Brain Res 2004;1004:1–7. [PubMed: 15033414]
6. Buijs RM, la Fleur SE, Wortel J, et al. The suprachiasmatic nucleus balances sympathetic and parasympathetic output to peripheral organs through separate preautonomic neurons. J Comp Neurol 2003;464:36–48. [PubMed: 12866127]
7. Glatzer NR, Hasney CP, Bhaskaran MD, et al. Synaptic and morphologic properties in vitro of premotor rat nucleus tractus solitarius neurons labeled transneuronally from the stomach. J Comp Neurol 2003;464:525–39. [PubMed: 12900922]
8. Cameron AA, Smith GM, Randall DC, et al. Genetic manipulation of intraspinal plasticity after spinal cord injury alters the severity of autonomic dysreflexia. J Neurosci 2006;26:2923–32. [PubMed: 16540569]
9. Hou S, Duale H, Cameron AA, et al. Plasticity of lumbosacral propriospinal neurons is associated with the development of autonomic dysreflexia after thoracic spinal cord transection. J Comp Neurol 2008;509:382–99. [PubMed: 18512692]
10. Karlsson AK. Autonomic dysreflexia. Spinal Cord 1999;37:383–91. [PubMed: 10432257]
11. Lindan R, Joiner E, Freehafer AA, et al. Incidence and clinical features of autonomic dysreflexia in patients with spinal cord injury. Paraplegia 1980;18:285–92. [PubMed: 7443280]
12. Krenz NR, Meakin SO, Krassioukov AV, et al. Neutralizing intraspinal nerve growth factor blocks autonomic dysreflexia caused by spinal cord injury. J Neurosci 1999;19:7405–14. [PubMed: 10460247]
13. Card JP, Rinaman L, Lynn RB, et al. Pseudorabies virus infection of the rat central nervous system: ultrastructural characterization of viral replication, transport, and pathogenesis. J Neurosci 1993;13:2515–39. [PubMed: 8388923]
14. Smith BN, Banfield BW, Smeraski CA, et al. Pseudorabies virus expressing enhanced green fluorescent protein: A tool for in vitro electrophysiological analysis of transsynaptically labeled neurons in identified central nervous system circuits. Proc Natl Acad Sci U S A 2000;97:9264–69. [PubMed: 10922076]
15. Campbell RE, Tour O, Palmer AE, et al. A monomeric red fluorescent protein. Proc Natl Acad Sci USA 2002;99:7877–82. [PubMed: 12060735]

NIH-PA Author Manuscript

NIH-PA Author Manuscript

NIH-PA Author Manuscript

16. Banfield BW, Kaufman JD, Randall JA, et al. Development of pseudorabies virus strains expressing red fluorescent proteins: new tools for multisynaptic labeling applications. J Virol 2003;77:10106–12. [PubMed: 12941921]

17. Jansen AS, Farwell DG, Loewy AD. Specificity of pseudorabies virus as a retrograde marker of sympathetic preganglionic neurons: implications for transneuronal labeling studies. Brain Res 1993;617:103–12. [PubMed: 8397044]

18. Ch'ng TH, Spear PG, Struyf F, et al. Glycoprotein D-independent spread of pseudorabies virus infection in cultured peripheral nervous system neurons in a compartmented system. J Virol 2007;81:10742–57. [PubMed: 17652377]

19. Pickard GE, Smeraski CA, Tomlinson CC, et al. Intravitreal injection of the attenuated pseudorabies virus PRV Bartha results in infection of the hamster suprachiasmatic nucleus only by retrograde transsynaptic transport via autonomic circuits. J Neurosci 2002;22:2701–10. [PubMed: 11923435]

20. Valentino RJ, Kosboth M, Colflesh M, et al. Transneuronal labeling from the rat distal colon: Anatomic evidence for regulation of distal colon function by a pontine corticotropin-releasing factor system. J Comp Neurol 2000;417:399–414. [PubMed: 10701863]

21. Anderson CR, Edwards SL. Intraperitoneal injections of Fluorogold reliably labels all sympathetic preganglionic neurons in the rat. J Neurosci Methods 1994;53:137–41. [PubMed: 7823616]

22. Zermann DH, Ishigooka M, Doggweiler-Wiygul R, et al. Central autonomic innervation of the kidney. What can we learn from a transneuronal tracing study in an animal model? J Urol 2005;173:1033–38. [PubMed: 15711371]

23. Weiss ML, Chowdhury SI, Patel KP, et al. Neural circuitry of the kidney: NO-containing neurons. Brain Res 2001;919:269–82. [PubMed: 11701139]

24. Huang J, Weiss ML. Characterization of the central cell groups regulating the kidney in the rat. Brain Res 1999;845:77–91. [PubMed: 10529446]

25. Guillery RW. On counting and counting errors. J Comp Neurol 2002;447:1–7. [PubMed: 11967890]

26. Abercrombie M. Estimation of nuclear population from microtome sections. Anat Rec 1946;94:239–47.

27. Sullivan PG, Rabchevsky AG, Keller JN, et al. Intrinsic differences in brain and spinal cord mitochondria: Implication for therapeutic interventions. J Comp Neurol 2004;474:524–34. [PubMed: 15174070]

28. Hamer DW, Santer RM. Anatomy and blood supply of the coeliac-superior mesenteric ganglion complex of the rat. Anat Embryol (Berl) 1981;162:353–62. [PubMed: 7270906]

29. Deng Y, Thompson BM, Gao X, et al. Temporal relationship of peroxynitrite-induced oxidative damage, calpain-mediated cytoskeletal degradation and neurodegeneration after traumatic brain injury. Exp Neurol 2007;205:154–65. [PubMed: 17349624]

30. Mettenleiter TC, Zsak L, Zuckermann F, et al. Interaction of glycoprotein gIII with a cellular heparinlike substance mediates adsorption of pseudorabies virus. J Virol 1990;64:278–86. [PubMed: 2152816]

31. Rauh I, Mettenleiter TC. Pseudorabies virus glycoproteins gII and gp50 are essential for virus penetration. J Virol 1991;65:5348–56. [PubMed: 1654444]

32. Card JP, Rinaman L, Schwaber JS, et al. Neurotropic properties of pseudorabies virus: uptake and transneuronal passage in the rat central nervous system. J Neurosci 1990;10:1974–94. [PubMed: 2162388]

33. Furlan JC, Fehlings MG, Shannon P, et al. Descending vasomotor pathways in humans: Correlation between axonal preservation and cardiovascular dysfunction after spinal cord injury. J Neurotrauma 2003;20:1351–63. [PubMed: 14748983]

34. Teasell RW, Arnold JM, Krassioukov A, et al. Cardiovascular consequences of loss of supraspinal control of the sympathetic nervous system after spinal cord injury. Arch Phys Med Rehabil 2000;81:506–16. [PubMed: 10768544]

35. Claus-Walker J, Halstead LS. Metabolic and endocrine changes in spinal cord injury: II (section 1). Consequences of partial decentralization of the autonomic nervous system. Arch Phys Med Rehabil 1982;63:569–75. [PubMed: 6753794]

36. Krassioukov AV, Weaver LC. Morphological changes in sympathetic preganglionic neurons after spinal cord injury in rats. Neuroscience 1996;70:211–25. [PubMed: 8848126]

NIH-PA Author Manuscript

NIH-PA Author Manuscript

NIH-PA Author Manuscript

37. Wallin BG, Stjernberg L. Sympathetic activity in man after spinal cord injury. Outflow to skin below the lesion. Brain 1984;107 (Pt 1):183–98. [PubMed: 6697155]
38. Maiorov DN, Weaver LC, Krassioukov AV. Relationship between sympathetic activity and arterial pressure in conscious spinal rats. Am J Physiol 1997;272:H625–31. [PubMed: 9124418]
39. Gattone VH 2nd, Marfurt CF, Dallie S. Extrinsic innervation of the rat kidney: a retrograde tracing study. Am J Physiol 1986;250:F189–96. [PubMed: 3753828]
40. de Groat WC, Kawatani M. Reorganization of sympathetic preganglionic connections in cat bladder ganglia following parasympathetic denervation. J Physiol 1989;409:431–49. [PubMed: 2573724]
41. Vizzard MA, Brisson M, de Groat WC. Transneuronal labeling of neurons in the adult rat central nervous system following inoculation of pseudorabies virus into the colon. Cell Tissue Res 2000;299:9–26. [PubMed: 10654066]
42. Pavcovich LA, Yang M, Miselis RR, et al. Novel role for the pontine micturition center, Barrington's nucleus: Evidence for coordination of colonic and forebrain activity. Brain Res 1998;784:355–61. [PubMed: 9518692]
43. Nauta HJ, Pritz MB, Lasek RJ. Afferents to the rat caudoputamen studied with horseradish peroxidase. An evaluation of a retrograde neuroanatomical research method. Brain Res 1974;67:219–38. [PubMed: 4143409]
44. Kuypers HG, Bentivoglio M, van der Kooy D, et al. Retrograde transport of bisbenzimide and propidium iodide through axons to their parent cell bodies. Neurosci Lett 1979;12:1–7. [PubMed: 88694]
45. Kuypers HG, Ugolini G. Viruses as transneuronal tracers. Trends Neurosci 1990;13:71–75. [PubMed: 1690933]
46. Ugolini G, Kuypers HG. Collaterals of corticospinal and pyramidal fibres to the pontine grey demonstrated by a new application of the fluorescent fibre labelling technique. Brain Res 1986;365:211–27. [PubMed: 2418921]
47. Su C, Na M, Chen J, et al. Gene-viral cancer therapy using dual-regulated oncolytic adenovirus with antiangiogenesis gene for increased efficacy. Mol Cancer Res 2008;6:568–75. [PubMed: 18344493]
48. Nicklin SA, Reynolds PN, Brosnan MJ, et al. Analysis of cell-specific promoters for viral gene therapy targeted at the vascular endothelium. Hypertension 2001;38:65–70. [PubMed: 11463761]
49. Ruitenberg MJ, Plant GW, Hamers FP, et al. Ex vivo adenoviral vector-mediated neurotrophin gene transfer to olfactory ensheathing glia: effects on rubrospinal tract regeneration, lesion size, and functional recovery after implantation in the injured rat spinal cord. J Neurosci 2003;23:7045–58. [PubMed: 12904465]

NIH-PA Author Manuscript
NIH-PA Author Manuscript
NIH-PA Author Manuscript

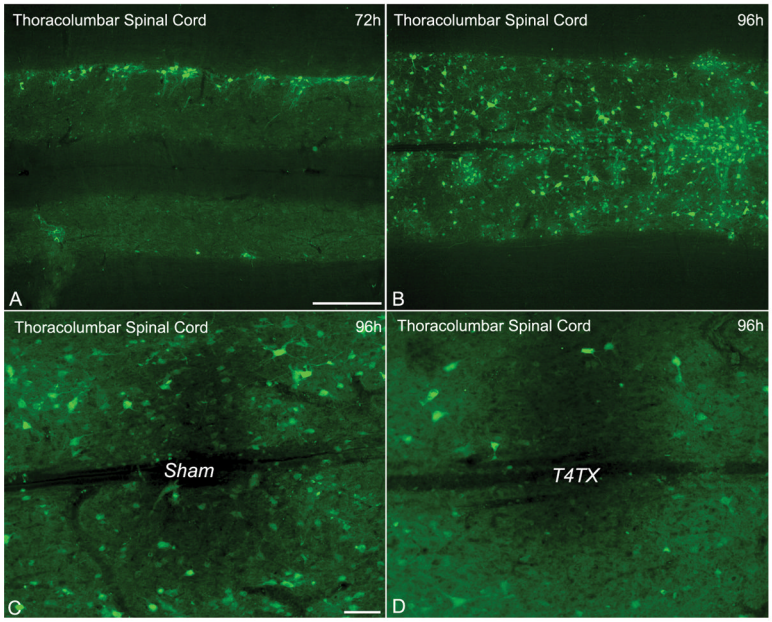

Figure 1.

(**A, B**) Photomicrographs representing the progression of PRV labeling of cells in the thoracolumbar spinal cord following PRV-152 inoculation into the left kidney of sham rats at 72 hours (**A**) and 96 hours (**B**) post-inoculation. The top of each panel represents the side of kidney injections. (**C, D**) Chronic spinal cord injury dramatically altered the PRV labeling pattern in (**C**) sham versus (**D**) T4-transected (T4TX) rats at 96 hours post-PRV-152 inoculation into the left kidney. Note the conspicuous diminished labeling after T4TX compared to the sham controls. Scale bars: **A, B** = 500 μm; **C, D** = 100 μm.

NIH-PA Author Manuscript

NIH-PA Author Manuscript

NIH-PA Author Manuscript

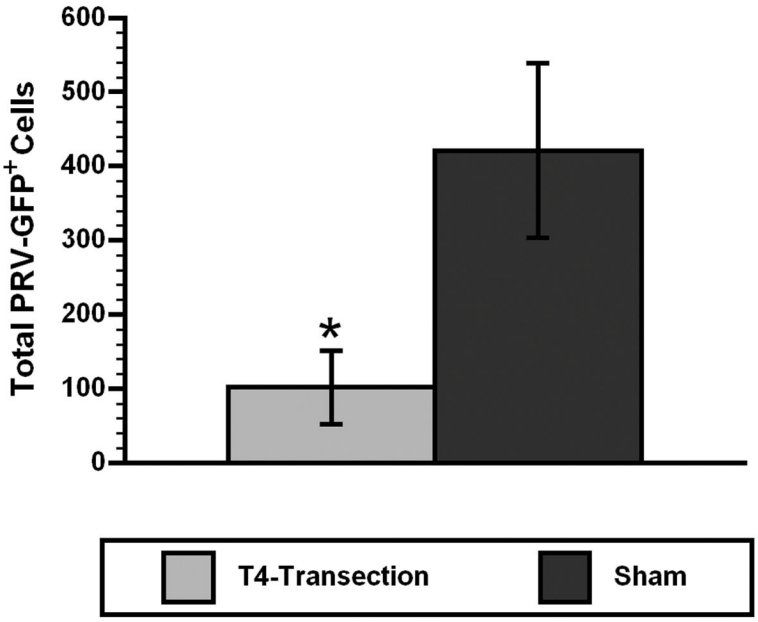

Figure 2.

Quantitative comparisons of EGFP$^+$ cells between T4-transected and sham rats throughout the thoracolumbar spinal cord (T8–T13) following PRV-152 injection into the left kidney at 96 hours post-inoculation. Bars represent mean ± SD. *$p < 0.01$.

NIH-PA Author Manuscript
NIH-PA Author Manuscript
NIH-PA Author Manuscript

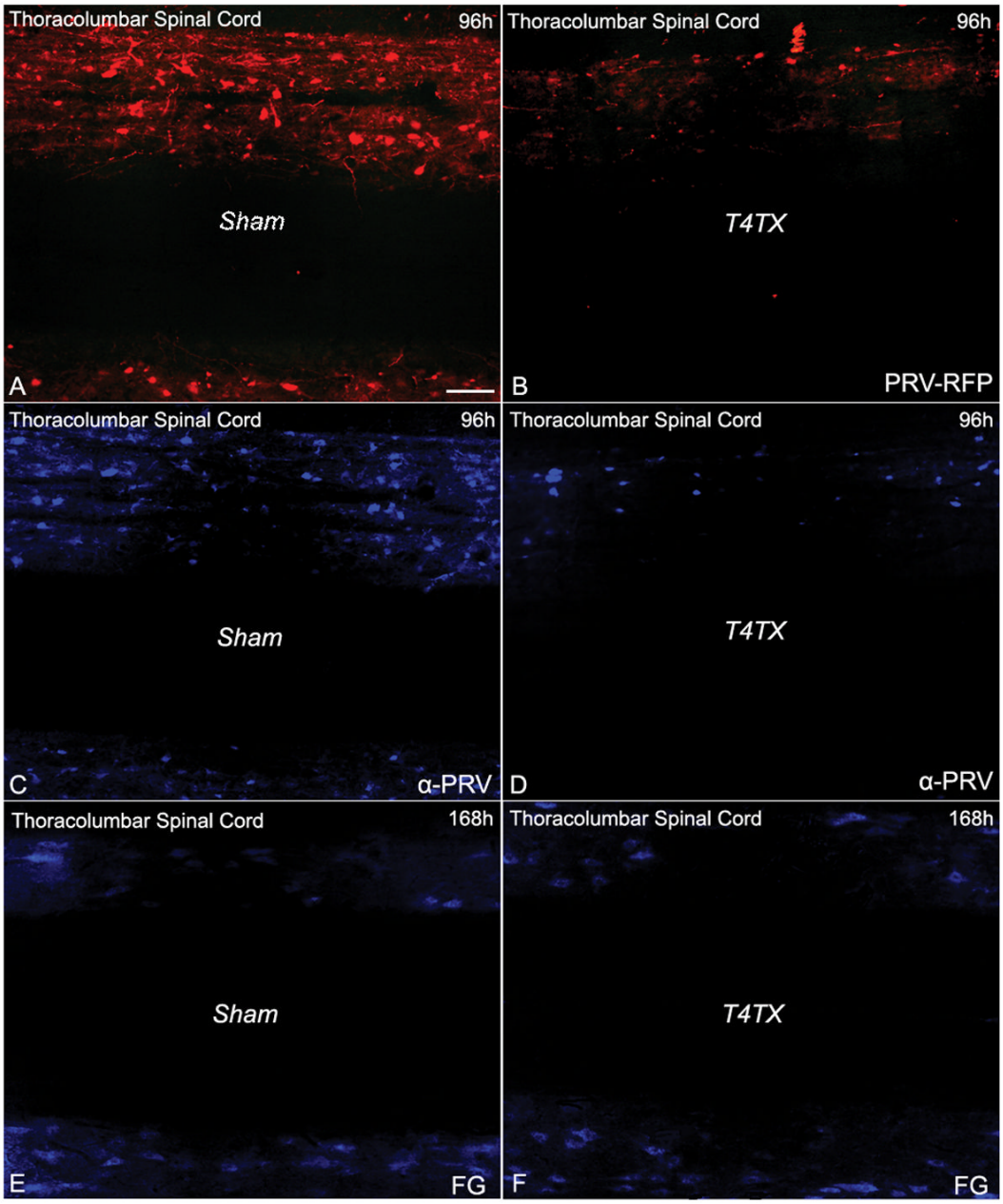

Figure 3.

Chronic T4-transection (T4TX) markedly decreased the PRV labeling pattern in the thoracolumbar spinal cord, irrespective of the reporter gene (PRV-152 or PRV-RFP) used in sham (**A**) versus T4TX (**B**) rats. Injury-induced aberrant PRV-RFP expression is in part due to compromised viral uptake since anti-PRV (α-PRV) double immunostaining in the same sections revealed more labeled neurons in sham (**C**) versus T4TX (**D**) rats. By contrast, FluoroGold (FG) labeling in the thoracolumbar spinal cord of (**E**) sham versus (**F**) chronic T4TX rats appeared unaltered. Scale bar = 100 μm and applies to all photographs.

NIH-PA Author Manuscript
NIH-PA Author Manuscript
NIH-PA Author Manuscript

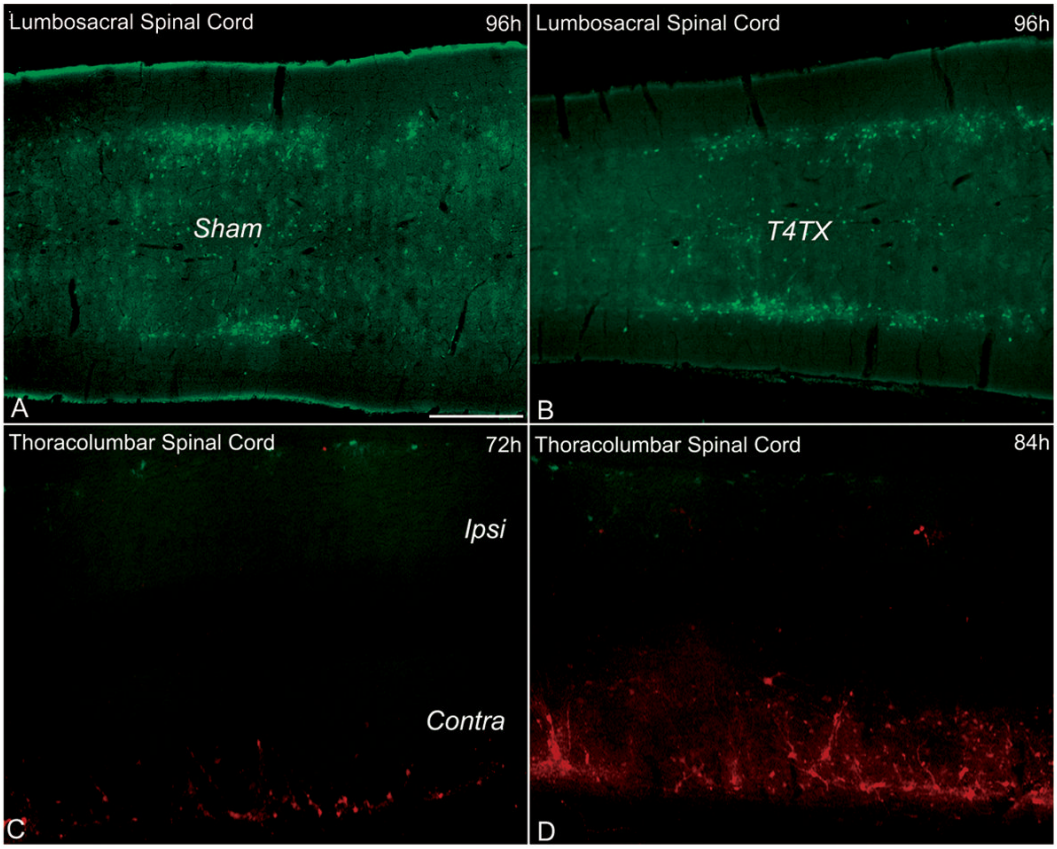

Figure 4.

Expression patterns of PRV-infected neurons in the lumbosacral (parasympathetic) and thoracolumbar (sympathetic) spinal cord following viral injections into the distal colon (**A**, **B**) or kidneys (**C**, **D**), respectively. Chronic T4-transection (T4TX) did not appear to affect PRV-152 uptake and/or expression patterns in sham (**A**) versus T4TX (**B**) rats at 96 hours post-inoculation. By contrast, left-sided T4-hemisected spinal cords (**C**, **D**) appeared to show reduced PRV-152 expression/uptake in the ipsilateral spinal cord (Ipsi) compared to PRV-614 labeling in the contralateral side (Contra) at 72 hours (**C**) and 84 hours (**D**) post-inoculation into the left kidney (PRV-152) and right kidney (PRV-614), respectively. Scale bar = 500 μm and applies to all panels.

NIH-PA Author Manuscript

NIH-PA Author Manuscript

NIH-PA Author Manuscript

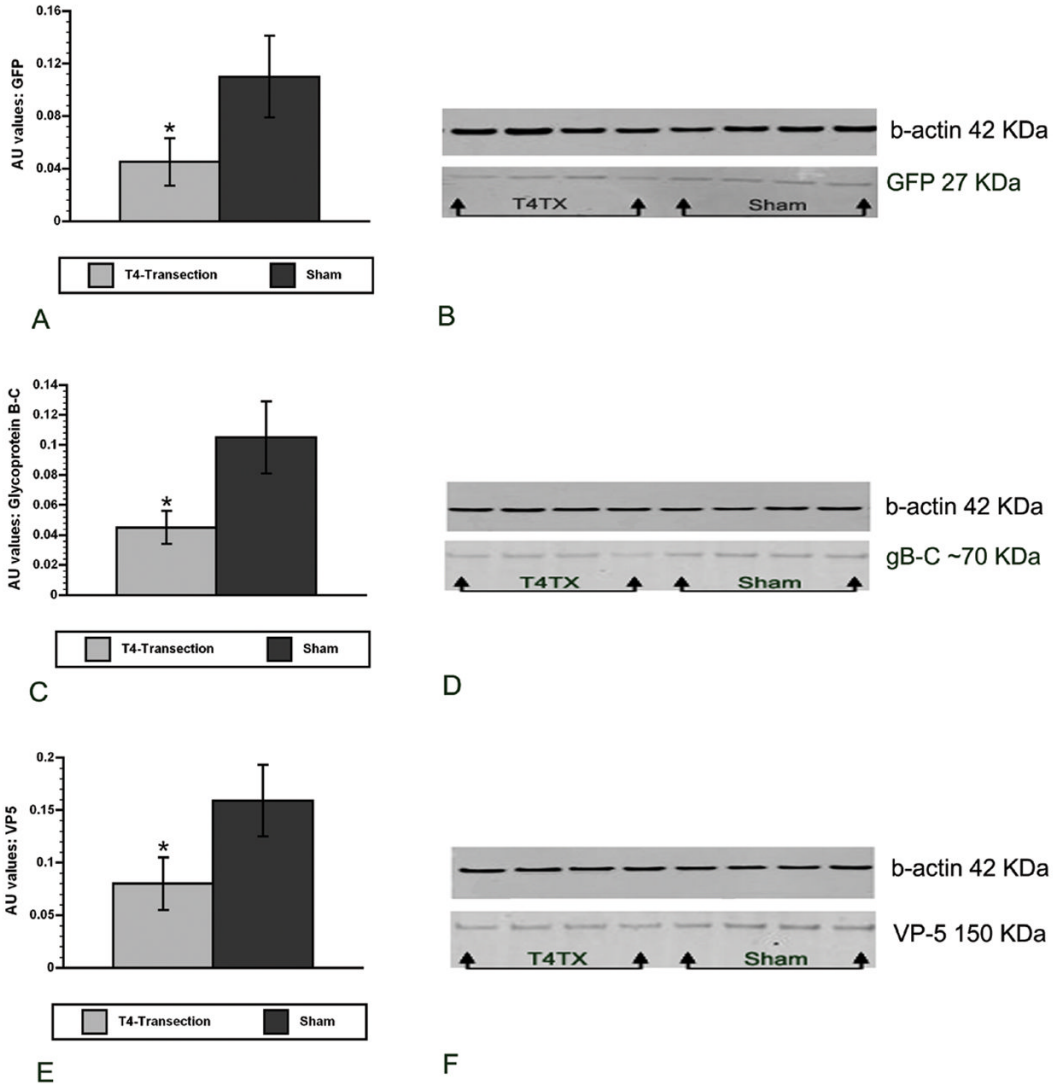

Figure 5.

Relative expression levels of EGFP and PRV-associated proteins in the thoracolumbar spinal cords of sham versus T4-transected (T4TX) rats. The dramatic reduction of PRV-152^{+} cells after injury in the thoracolumbar spinal cord was corroborated by Western blot analysis of (**A**) EGFP protein levels (arbitrary unit; AU) in T4TX versus sham rats at 96 hours post-PRV-152 inoculation into the left kidney. (**B**) Protein blots (EGFP and β-actin) from T4TX versus sham rats. (**C**) Viral glycoprotein B–C (gB–C) expression levels (AU), an important component for host-cell adsorption and entry, were significantly reduced in T4TX versus sham rats at 96h post-PRV-152 inoculation. (**D**) Protein blots (gB–C and β-actin) from T4TX versus sham rats. (**E**) The expression levels of major capsid coat protein (VP-5; AU), an important element in the construction of the PRV capsid, was significantly reduced in T4TX versus sham rats at 96 hours post-PRV-152 inoculation. (**F**) Protein blots (VP-5 and β-actin) from T4TX versus sham rats. Bars represent mean ± SD. *$p < 0.01$.

NIH-PA Author Manuscript

NIH-PA Author Manuscript

NIH-PA Author Manuscript

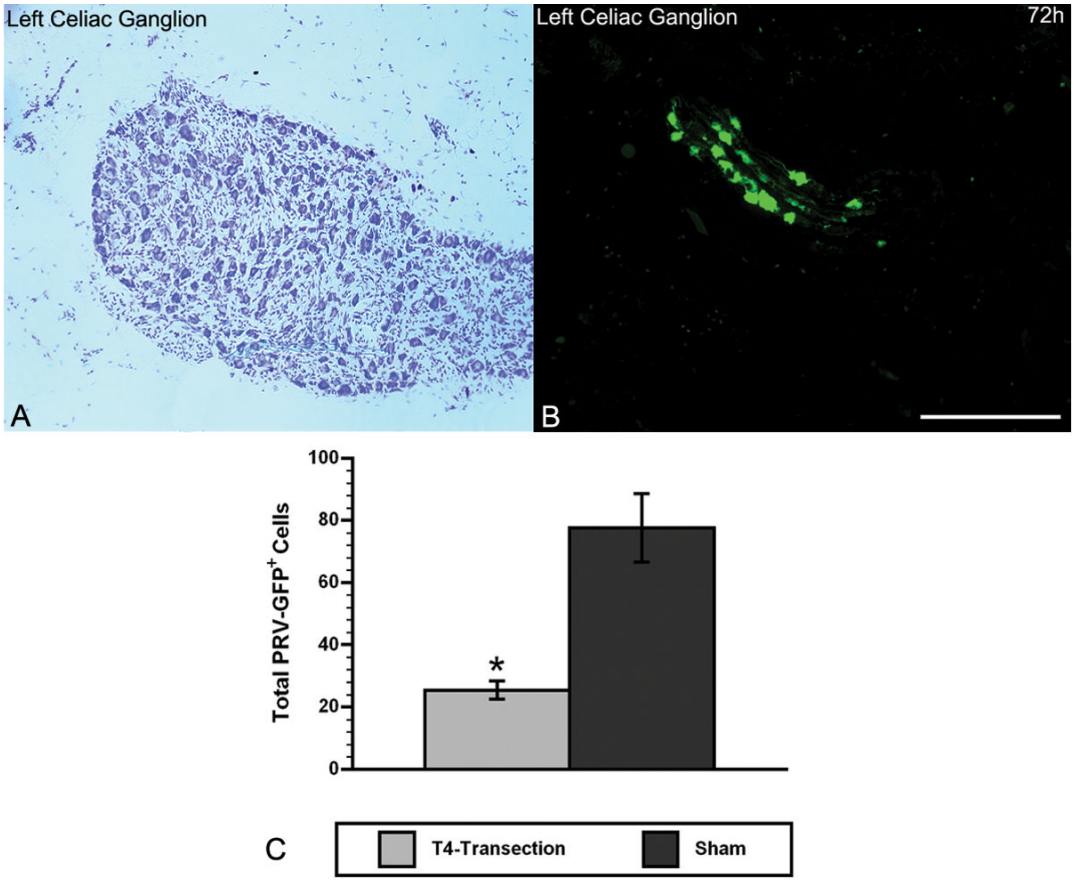

Figure 6.

Photomicrographs of cresyl violet stained left celiac ganglion (**A**) and PRV labeling pattern in left celiac ganglion following PRV-152 inoculation into left kidney of a sham rat (**B**) at 72 hours. A subpopulation of celiac ganglionic neurons innervates the kidneys. Scale bar = 200 μm and applies to both images. **(C)** Quantitative comparison of $EGFP^+$ cells between T4-transected and sham rats in the left celiac ganglia following PRV-152 injection into the left kidney at 72 hours post-inoculation. Bars represent mean ± SD. *$p < 0.01$.

NIH-PA Author Manuscript

NIH-PA Author Manuscript

NIH-PA Author Manuscript

Table 1

Total Number of Rats Used in the Different Experimental Paradigms

Injection Groups	T4-transection	T4-hemisection	Sham	Naive
PRV-GFP; left kidney (n = 39)	18	3	18	-
PRV-GFP; right kidney (n = 3)	-	3	-	-
PRV-GFP; distal colon (n = 6)	3	-	3	-
PRV-RFP; left kidney (n = 9)	3	3	3	-
PRV-RFP; right kidney (n = 3)	-	3	-	-
FluoroGold; intraperitoneal (n = 4)	2	-	2	-
PRV specificity control (n= 2)	-	-	-	2
Total (n = 66)	**26**	**12**	**26**	**2**

PRV, Pseudorabies virus; GFP, green fluorescent protein; RFP, red fluorescent protein.

NIH-PA Author Manuscript

NIH-PA Author Manuscript

NIH-PA Author Manuscript

Table 2

Celiac Ganglia and Spinal Tissues Used in the Different Experimental Groups

Experimental paradigm	T4-transection	T4-hemisection	Sham	Naive
Histology: 48 hours post-PRV inoculation[#]	3	-	3	-
Histology: 72 hours post-PRV inoculation [*#]	5	4	5	-
Histology: 84 hours post-PRV inoculation [*]	2	4	2	-
Histology: 96 hours post-PRV inoculation [*]	10	4	10	2
Histology: 168 hours post-FG injection	2	-	2	-
Western blot analysis: 96 hours post-PRV inoculation	4	-	4	-
Total (n = 66)	**26**	**12**	**26**	**2**

[*] Includes both PRV-152 (green) and PRV-614 (red).

[#] Includes celiac ganglia.

PRV, pseudorabies virus; FG, FluoroGold.